J|A|C|S
ARTICLES
Published on Web 08/10/2002

Ultrafast UV Pump/IR Probe Studies of C−H Activation in Linear, Cyclic, and Aryl Hydrocarbons

Matthew C. Asplund,† Preston T. Snee, Jake S. Yeston,‡ Matthew J. Wilkens, Christine K. Payne, Haw Yang, Kenneth T. Kotz, Heinz Frei,* Robert G. Bergman,* and Charles B. Harris*

Contribution from the Department of Chemistry, University of California, Berkeley, California 94720, and Chemical Sciences Division and Physical Biosciences Division, Ernest Orlando Lawrence Berkeley, National Laboratory, Berkeley, California 94720

Received March 21, 2002

Abstract: The photochemical C−H activation reactions of η^3-Tp*Rh(CO)$_2$ (Tp* = HB−Pz$_3$*, Pz* = 3,5-dimethylpyrazolyl) and CpRh(CO)$_2$ (Cp = C_5H_5) have been studied in a series of linear, cyclic, and aromatic hydrocarbon solvents on a femtosecond to microsecond time scale. These results have revealed that the structure of the hydrocarbon substrate affects the final C−H bond activation step, which is in accordance with the known preference of bond activation toward primary C−H sites. In the case of aromatic C−H activation, the reaction is divided into parallel channels involving σ- and π-solvated intermediates. Results for the analogous CpRh(CO)$_2$ molecule have shown that the coordination of the cyclopentadienyl ligand does not play a direct role in the dynamics of the reaction, in contrast to the C−H activation mechanism observed in η^3-Tp*Rh(CO)$_2$ studies.

Introduction

The C−H bond activation reaction by transient organometallic species has been the subject of great interest in the chemical sciences.[1−7] Previously, we reported our results on the photochemical C−H activation mechanism of η^3-Tp*Rh(CO)$_2$ (Tp* = HB−Pz*$_3$, Pz* = 3,5-dimethylpyrazolyl),[8,9] which is known to form stable C−H activated products upon photolysis with appreciable quantum efficiency.[10−12] These findings are summarized in Scheme 1. While the previous work focused on the ligand dynamics, it is also important to assess the role of the structure of the hydrocarbon substrate in the activation process. A number of recent studies have addressed this issue for related transition metal systems, although none have focused on ultrafast time scales.[13−15]

It has been proposed that C−H activation by group 9 coordinatively unsaturated complexes is fundamentally a two-step process.[6,16−19] The first step (coordination) involves loose binding of the hydrocarbon to the metal center, while the second step (insertion) involves scission of the C−H bond and formation of new metal carbon M−C and metal hydride M−H bonds. In the coordination step, saturated alkanes form σ-complexes through interaction of the metal with a C−H bond. Olefins and aromatic compounds can also bind to the metal center through the π-electrons of the double bonds.[20−30] The

* Address correspondence to these authors. E-mail: Heinz Frei, HMFrei@lbl.gov; Robert G. Bergman, bergman@cchem.berkeley.edu; Charles B. Harris, harris@socrates.berkeley.edu.

† Present address: Department of Chemistry and Biochemistry, Brigham Young University, Provo, UT 84602.

‡ Present address: NIST, Gaithersburg, MD 20899-8441.

(1) Arndtsen, B. A.; Bergman, R. G.; Mobley, T. A.; Peterson, T. H. *Acc. Chem. Res.* **1995**, *28*, 154.
(2) Crabtree, R. H. *Chem. Rev.* **1985**, *85*, 245.
(3) *Activation and Functionalization of Alkanes*; Hill, C. L., Ed.; Wiley: New York, 1989.
(4) Wasserman, E. P.; Moore, C. B.; Bergman, R. G. *Science* **1992**, *255*, 315.
(5) Shilov, A. E.; Shul'pin, G. B. *Activation and Catalytic Reactions of Saturated Hydrocarbons in the Presence of Metal Complexes*; Kluwer: Boston, 2000.
(6) Stahl, S. S.; Labinger, J. A.; Bercaw, J. E. *Angew. Chem., Int. Ed. Engl.* **1998**, *37*, 2181.
(7) Shilov, A. E.; Shul'pin, G. B. *Chem. Rev.* **1997**, *97*, 2879.
(8) Lian, T.; Bromberg, S. E.; Yang, H.; Proulx, G.; Bergman, R. G.; Harris, C. B. *J. Am. Chem. Soc.* **1996**, *118*, 3769.
(9) Bromberg, S. E.; Yang, H.; Asplund, M. C.; Lian, T.; McNamara, B. K.; Kotz, K. T.; Yeston, J. S.; Wilkens, M. J.; Frei, H.; Bergman, R. G.; Harris, C. B. *Science* **1997**, *278*, 260.
(10) Ghosh, C. K.; Graham, W. A. G. *J. Am. Chem. Soc.* **1987**, *109*, 4726.
(11) Bloyce, P. E.; Mascetti, J.; Rest, A. J. *J. Organomet. Chem.* **1993**, *444*, 223.
(12) Purwoko, A. A.; Lees, A. J. *Inorg. Chem.* **1995**, *34*, 424.
(13) Northcutt, T. O.; Wick, D. D.; Vetter, A. J.; Jones, W. D. *J. Am. Chem. Soc.* **2001**, *123*, 7257.
(14) Bennett, J. L.; Wolczanski, P. T. *J. Am. Chem. Soc.* **1997**, *119*, 10696.
(15) McNamara, B. K.; Yeston, J. S.; Bergman, R. G.; Moore, C. B. *J. Am. Chem. Soc.* **1999**, *121*, 6437.
(16) Wick, D. D.; Reynolds, K. A.; Jones, W. D. *J. Am. Chem. Soc.* **1999**, *121*, 3974.
(17) Mobley, T. A.; Schade, C.; Bergman, R. G. *Organometallics* **1998**, *17*, 3574.
(18) Gross, C. L.; Girolami, G. S. *J. Am. Chem. Soc.* **1998**, *120*, 6605.
(19) Schafer, D. F.; Wolczanski, P. T. *J. Am. Chem. Soc.* **1998**, *120*, 4881.
(20) Jones, W. D.; Feher, F. J. *J. Am. Chem. Soc.* **1986**, *108*, 4814.
(21) Jones, W. D.; Feher, F. J. *J. Am. Chem. Soc.* **1982**, *104*, 4240.
(22) Jones, W. D.; Feher, F. J. *Acc. Chem. Res.* **1989**, *22*, 91.
(23) Parshall, G. W. *Acc. Chem. Res.* **1970**, *3*, 139.
(24) Muetterties, E. L.; Bleeke, J. R. *Acc. Chem. Res.* **1979**, *12*, 324.
(25) Nubel, P. O.; Brown, T. L. *J. Am. Chem. Soc.* **1984**, *106*, 644.
(26) Gunnoe, T. B.; Sabat, M.; Harman, W. D. *J. Am. Chem. Soc.* **1998**, *120*, 8747.
(27) Meiere, S. H.; Brooks, B. C.; Gunnoe, B. T.; Carrig, E. H.; Sabat, M.; Harman, W. D. *Organometallics* **2001**, *20*, 3361.
(28) Belt, S. T.; Dong, L.; Duckett, S. B.; Jones, W. D.; Partridge, M. G.; Perutz, R. N. *J. Chem. Soc., Chem. Commun.* **1991**, 266.
(29) Chin, R. M.; Dong, L.; Duckett, S. B.; Partridge, M. G.; Jones, W. D.; Perutz, R. N. *J. Am. Chem. Soc.* **1993**, *115*, 7685.

Scheme 1. C−H Bond Activation Mechanism of η^3-Tp*Rh(CO)$_2$ in Linear and Cyclic Hydrocarbons

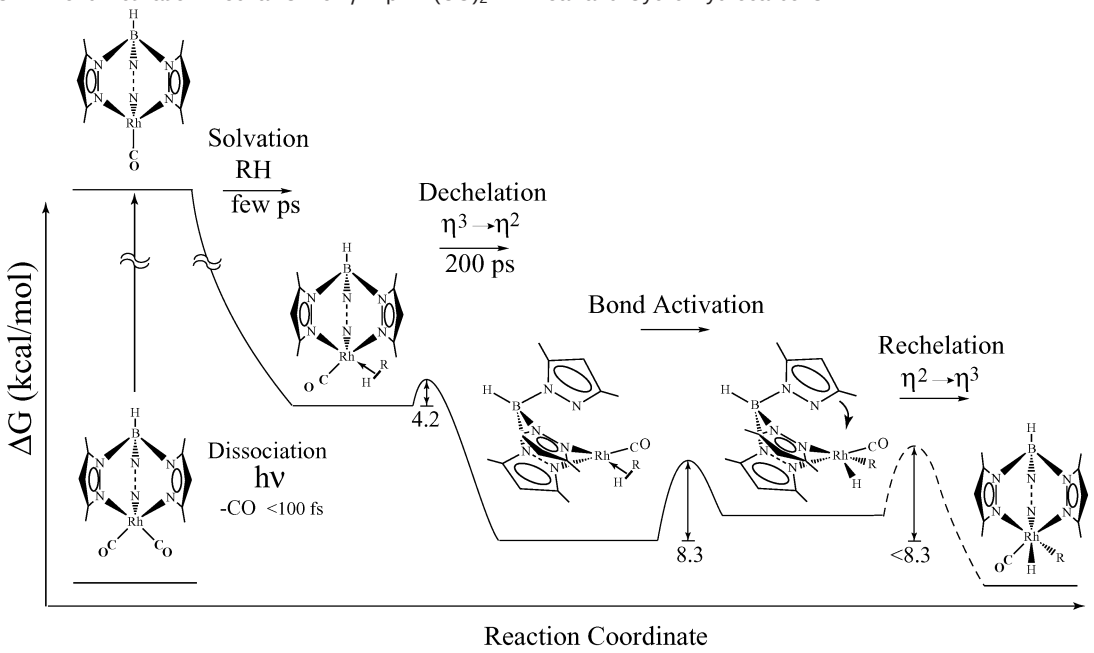

role of such π-complexes in C−H activation of unsaturated hydrocarbons has not been entirely resolved.[31]

The insertion step has been studied in great detail. Bergman and co-workers have shown that for reaction of hydrocarbons at the unsaturated Cp*Rh(CO) (Cp* = $C_5(CH_3)_5$) center in low-temperature liquid Kr, insertion proceeds 2−10 times more rapidly for linear alkanes than for the comparable saturated cyclic substrates.[15] In a similar vein, Jones and co-workers have recently shown that the relative barrier for insertion at the Tp*Rh(CNCH$_2$C(CH$_3$)$_3$) center increases in the order methane < primary C−H < secondary C−H.[13] The conclusions presented in this paper, which are based upon direct ultrafast observation of all the reactive intermediates, will shed more light on the generality of the previous findings.

Due to the reactivity of the intermediates, it is necessary to use ultrafast UV pump/IR probe methods to observe the reaction dynamics of photoproducts under ambient conditions. We have used these methods to study the role of the substrate structure in C−H bond activation reactions at Rh centers. The results elucidate the photochemical dynamics of η^3-Tp*Rh(CO)$_2$ in linear, cyclic, and aromatic hydrocarbons on a femtosecond to microsecond time scale. The photochemistry of CpRh(CO)$_2$ (Cp = C_5H_5) in linear alkanes has also been examined to provide a basis of comparison to the Tp*Rh(CO)$_2$ studies.

Experimental Section

Sample Synthesis/Sample Handling. The compounds η^3-Tp*Rh(CO)$_2$ and η^2-Bp*Rh(CO)$_2$ were synthesized according to published procedures.[32−34] The compound CpRh(CO)$_2$ was synthesized from [RhCl(CO)$_2$]$_2$ and TlC_5H_5 using a previously published method.[35,36] Sample solutions were made under a controlled atmosphere in an airtight, demountable IR flow cell (Harrick Scientific Corp.). The purity of the samples was established using standard spectroscopic methods.

Femtosecond Infrared Spectroscopy. The system used to measure femtosecond spectra and kinetics has been described previously.[37] Femtosecond laser pulses are generated in our system by amplifying the output of a Ti:sapphire oscillator in two prism-bored dye cells which are pumped by the output of a frequency-doubled 30 Hz Nd:YAG laser. The amplified light centered at ~810 nm was then split into three beams. One beam was further amplified to give 70 fs, 7 μJ pulses, while the other two were focused into two sapphire windows to generate a white light continuum. Desired wavelengths of the white light were selected by two band-pass filters with a full width at half-maximum (fwhm) of 10 nm and further amplified by three-stage dye amplifiers to produce light pulses centered at 590 or 650 nm, as well as 690 nm. In this study, the excitation pulses of 295 or 325 nm were generated by frequency doubling the 590 or 650 nm light, respectively. The resulting UV photons (with energy of ~4 μJ/pulse) were focused into a disk of ~200 μm diameter at the sample to initiate the chemical reactions. The required time delay between a pump pulse and a probe pulse was achieved by guiding the pump beam through a variable delay line.

The broadband, ultrafast probe pulses centered at 5 μm were generated by mixing the 690 nm beam with the 810 nm beam. The resulting ~5 μJ IR pulses having temporal fwhm of about 70 fs and spectral bandwidth of about 200 cm^{-1} were split into a signal and a reference beam. Some data have been collected using an older system consisting of a monochromator with matched dual single element HgCdTe detectors,[37] while other data were collected by focusing the signal and reference beams into an astigmatism-corrected spectrographic monochromator to form two spectrally resolved images on a focal-plane-array detector.[38] The typical spectral and temporal resolution for these setups are 4 cm^{-1} and 300 fs, respectively. The polarizations of the pump and the probe pulse were set at the magic angle (54.7°) to ensure that all signals were due to population dynamics. A broad, wavelength-independent background signal from CaF_2 windows has been subtracted from the transient spectra and kinetic traces.

(30) Reinartz, S.; White, P. S.; Brookhart, M.; Templeton, J. L. *J. Am. Chem. Soc.* **2001**, *123*, 12724.
(31) There is evidence that C−H activation in ethylene by Cp*IrPMe$_3$ does not necessarily occur through prior formation of a π-complex. See: Stoutland, P. O.; Bergman, R. G. *J. Am. Chem. Soc.* **1985**, *107*, 4581.
(32) Trofimenko, S. *J. Am. Chem. Soc.* **1967**, *89*, 6288.
(33) May, S.; Reinsalu, P.; Powell, J. *Inorg. Chem.* **1980**, *19*, 1582.
(34) Bonati, F.; Mingetti, G.; Banditelli, G. *J. Organomet. Chem.* **1975**, *87*, 365.
(35) Knight, J.; Mays, J. *J. Chem. Soc. A* **1970**, 654.
(36) Snee, P. T.; Payne, C. K.; Kotz, K. T.; Yang, H.; Harris, C. B. *J. Am. Chem. Soc.* **2001**, *123*, 2255.
(37) Lian, T.; Bromberg, S. E.; Asplund, M. C.; Yang, H.; Harris, C. B. *J. Phys. Chem.* **1996**, *100*, 11994.
(38) Yang, H.; Snee, P. T.; Kotz, K. T.; Payne, C. K.; Frei, H.; Harris, C. B. *J. Am. Chem. Soc.* **1999**, *121*, 9227.

Nanosecond Step-Scan Fourier Transform Infrared (FTIR) Spectroscopy. These measurements were made using a nanosecond step-scan interferometer described elsewhere.[39] The instrument is based on a Bruker IFS-88 FTIR with a special scanner module to allow step-scanning. An InSb detector with a 40 ns fwhm response measured from the IR scatter of 1064 nm light from a YAG laser was used. The IR light was focused in the sample compartment with two 10 mm focal length BaF_2 lenses, which gave beam sizes smaller than those given by comparable curved mirrors, allowing increased IR throughput and less sample degradation. The sample was photoexcited with 10 ns pulses from either the fourth harmonic output of a YAG laser or the second harmonic of a dye laser tuned to 590 nm. The early time data in some experiments are affected by transient heating of the sample during the course of the experiment. This thermal effect has the result of reducing the absolute time response of the system from ~40 to ~100 ns as discussed below.

Quantum Chemical Modeling. To compare single point energies consistently, all calculations were carried out using density functional theory (DFT) optimized geometries. The hybrid B3LYP functional was used for the DFT calculations with the Gaussian 98 suite of packages.[40–42] These calculations were run at the Ira and Marylou Fulton Supercomputer Center at Brigham Young University. The basis set consisted of the 6-31G basis functions for H, C, O, and P[43,44] and the Los Alamos effective core potential (ECP) for Rh with the outermost core orbitals included in the valence description.[45] All geometry optimizations of the model intermediate complexes η^2-Tp*Rh(CO) with CH_4 and C_6H_6 were followed by a frequency analysis to make certain that the optimized geometries were at a minimum. Interaction energies were calculated using the counterpoise method to account for basis set superposition error.[46,47]

Results

1. Tp*Rh(CO)$_2$ in Linear and Cyclic Hydrocarbons. The photochemical C−H activation reaction of η^3-Tp*Rh(CO)$_2$ in *n*-pentane and *n*-hexane as well as in cyclopentane and cyclohexane has been investigated in detail. The results of these studies have shown that the dynamics are divided between picosecond and nanosecond to microsecond time scale components. On the early picosecond time scale, the spectral data indicate that there is very little difference in the reactivity between linear and cyclic alkanes. After the initial photochemical CO loss, the coordinatively unsaturated complex is solvated by a C−H bond to form a σ-complexed intermediate. After 200 ps, the Tp* ligand dechelates to form an η^2 species as confirmed by analogous studies with η^2-Bp*Rh(CO)(alkane) (Bp* = H_2-BPz_2*) and by theoretical calculations.[9,48] This process is illustrated in Scheme 1.

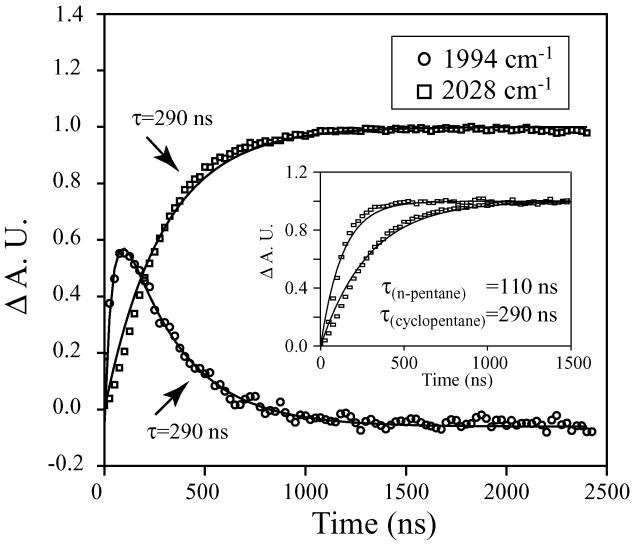

Figure 1. Transient kinetics of the intermediate η^2-Tp*Rh(CO)(solvent) (circles) and product η^3-Tp*Rh(CO)(H)(R) (squares) observed in cyclopentane. The inset shows the product kinetics in pentane and cyclopentane. (A. U. = arbitrary units.)

It is in the nanosecond time scale that differences are noted between linear and cyclic hydrocarbons. Shown in Figure 1 are the nanosecond kinetics of the intermediate η^2-Tp*Rh(CO)-(C_5H_{10}) and the final product η^3-Tp*Rh(CO)(H)(C_5H_9) in cyclopentane. The data indicate that the alkyl-solvated η^2-Tp*Rh(CO)(C_5H_{10}) species observed at 1994 cm^{-1} decays with a concomitant rise in the bond-activated product absorbing at 2028 cm^{-1} with a time scale of 290 ns. Shown in the inset of the figure are the kinetic traces of the C−H bond activated products in *n*-pentane and cyclopentane. The formation of the product in the linear alkane solvent has a much faster growth of less than 110 ns, and an intermediate η^2 species is difficult to observe.[49] Nanosecond experiments in *n*-hexane and cyclohexane show a faster formation of the product in the linear alkane as compared to the cyclic counterpart.[50] Using simple transition state theory, the corresponding free energy barrier for the activation step may be estimated as lying between 6.0 and 7.8 kcal/mol for linear alkanes and 8.4 kcal/mol for C−H activation of cyclic hydrocarbons.

To explore the differences between linear and cyclic hydrocarbons further, the reaction of η^3-Tp*Rh(CO)$_2$ in methylcyclohexane was examined. It was found that the time scale of the final activation step is similar to that observed in linear alkanes. Analogous results were obtained in mixed linear/cyclic alkane solvents: the observed product formation time scale is reduced by ~50% in a solution of 0.1 mol fraction *n*-pentane in cyclopentane relative to the product formation time scale in neat cyclopentane.[50]

To establish the magnitude of the kinetic isotope effect, the activation time scale has been measured using d_{12}-cyclohexane.

(39) Sun, H.; Frei, H. *J. Phys. Chem. B* **1997**, *101*, 205.
(40) Becke, A. D. *J. Chem. Phys.* **1993**, *98*, 5648.
(41) Lee, C.; Yang, W.; Parr, R. G. *Phys. Rev.* **1998**, *B41*, 785.
(42) Frisch, M. J.; Trucks, G. W.; Schlegel, H. B.; Scuseria, G. E.; Robb, M. A.; Cheeseman, J. R.; Zakrzewski, V. G.; Montgomery, J. A., Jr.; Stratmann, R. E.; Burant, J. C.; Dapprich, S.; Millam, J. M.; Daniels, A. D.; Kudin, K. N.; Strain, M. C.; Farkas, O.; Tomasi, J.; Barone, V.; Cossi, M.; Cammi, R.; Mennucci, B.; Pomelli, C.; Adamo, C.; Clifford, S.; Ochterski, J.; Petersson, G. A.; Ayala, P. Y.; Cui, Q.; Morokuma, K.; Malick, D. K.; Rabuck, A. D.; Raghavachari, K.; Foresman, J. B.; Cioslowski, J.; Ortiz, J. V.; Stefanov, B. B.; Liu, G.; Liashenko, A.; Piskorz, P.; Komaromi, I.; Gomperts, R.; Martin, R. L.; Fox, D. J.; Keith, T.; Al-Laham, M. A.; Peng, C. Y.; Nanayakkara, A.; Gonzalez, C.; Challacombe, M.; Gill, P. M. W.; Johnson, B. G.; Chen, W.; Wong, M. W.; Andres, J. L.; Head-Gordon, M.; Replogle, E. S.; Pople, J. A. *Gaussian 98*, revision A.9; Gaussian, Inc.: Pittsburgh, PA, 1998.
(43) Hehre, W. J.; Ditchfield, R.; Pople, J. A. *J. Chem. Phys.* **1972**, *56*, 2257.
(44) Francl, M. M.; Petro, W. J.; Hehre, W. J.; Binkley, J. S.; Gordon, M. S.; Defrees, D. J.; Pople, J. A. *J. Chem. Phys.* **1982**, *77*, 3654.
(45) Hay, P. J.; Wadt, W. R. *J. Chem. Phys.* **1985**, *82*, 299.
(46) Boys, S. F.; Bernardi, F. *Mol. Phys.* **1970**, *19*, 553.
(47) The zero point energy (ZPE) correction has not been applied to the calculated binding strengths; however, the correction is usually on the order of +1 kcal/mol.
(48) Zaric, S.; Hall, M. B. *J. Phys. Chem.* **1998**, *102*, 1963.
(49) The rate at which the C−H bonds in linear alkanes are activated may be greater than the ~120 ns observed in the present studies due to thermal effects discussed in the Experimental Section. As the product is not observed in the femtosecond studies, we may conclude that the C−H bond in linear alkanes is activated within ~5 to ~100 ns, which corresponds to a free energy barrier between 6.0 and 7.8 kcal/mol. Consequently, activation in linear hydrocarbons may be more favorable than that in their cyclic counterparts than the data imply.
(50) Asplund, M. C. In *Time-Resolved Infrared Studies of C−H Bond Activation by Organometallics*; University of California at Berkeley: Berkeley, CA, 1998.

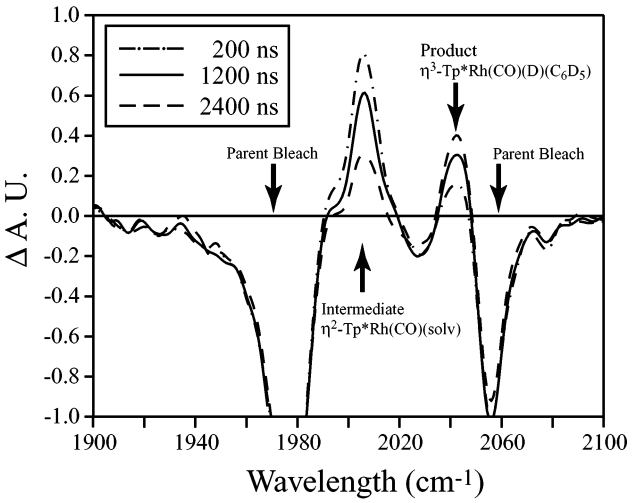

Figure 2. Transient difference spectra in the CO stretching region for η^3-Tp*Rh(CO)$_2$ in neat d_6-benzene at 200, 1200, and 2400 ns following UV photolysis. (A. U. = arbitrary units.)

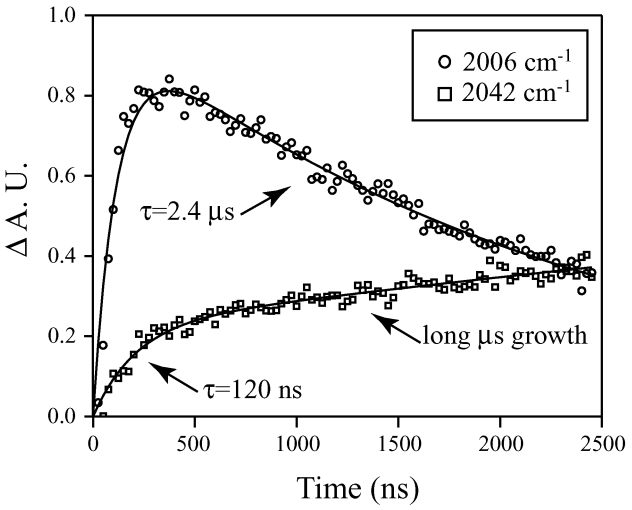

Figure 3. Ultrafast kinetics of the intermediate η^2-Tp*Rh(CO)(solvent) (circles) and product η^3-Tp*Rh(CO)(H)(R) (squares) in d_6-benzene. The time constants for the exponential fits (solid lines) are shown in the graph. (A. U. = arbitrary units.)

It was found that the formation of the final product in the deuterated solvent has a 520 ns growth, compared to the 230 ns time scale observed in cyclohexane.

2. Tp*Rh(CO)$_2$ in Aromatic Hydrocarbons. The C−H activation reaction of η^3-Tp*Rh(CO)$_2$ in d_6-benzene and toluene has also been studied. At early times, the femtosecond d_6-benzene spectra indicate that the C−H activation mechanism is not significantly altered in aromatic solvents. The data show that the solvated monocarbonyl appears at 1965 cm^{-1} and decays in ~200 ps to form a new intermediate absorbing at 2006 cm^{-1}. The ultrafast time-resolved spectra are given in the Supporting Information. Shown in Figure 2 are the nanosecond spectra of η^3-Tp*Rh(CO)$_2$ in d_6-benzene. The intermediate absorbing at 2006 cm^{-1} decays on a 2.4 ± 0.2 μs time scale with a concomitant rise in the bond-activated product η^3-Tp*Rh(CO)(D)(C$_6$D$_5$) absorbing at 2042 cm^{-1} as shown in the kinetic traces in Figure 3. The kinetics of the C−D activated product's growth monitored at 2042 cm^{-1} are biexponential, with a fast (less than 120 ns) rise and a longer microsecond growth component. Unfortunately, the microsecond component of the product's rise

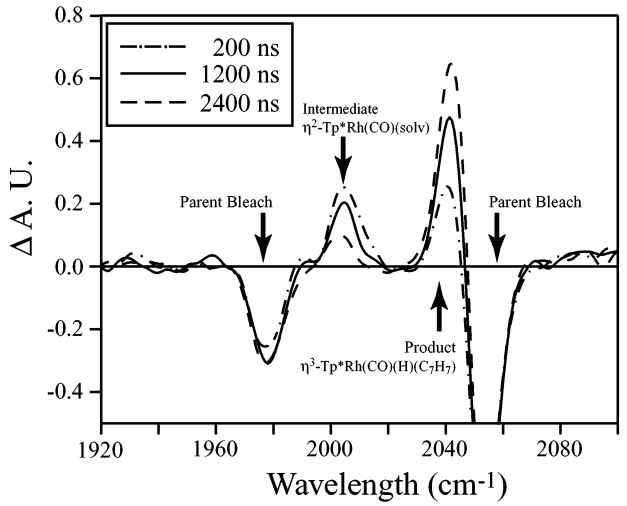

Figure 4. Transient difference spectra in the CO stretching region for η^3-Tp*Rh(CO)$_2$ in neat toluene at 200, 1200, and 2400 ns following UV photolysis. (A. U. = arbitrary units.)

time is difficult to accurately fit due to the fact that the absolute longtime absorption under the experimental conditions is not known. Despite this, the decay of the intermediate absorbing at 2006 cm^{-1} is strongly correlated to the microsecond rise of the product and this decay time scale is a meaningful representation of the product formation kinetics. The barrier from transition state theory for the C−D activation step is thus calculated to be 9.6 kcal/mol. The faster component of the product's kinetics may be attributed to product formation from an unobserved intermediate, as discussed below.

Shown in Figure 4 are the nanosecond spectra of η^3-Tp*Rh(CO)$_2$ in toluene. These data are almost identical to the d_6-benzene results; the intermediate species seen at 2005 cm^{-1} decays along a slightly faster 2.1 ± 0.1 μs time scale. The product η^3-Tp*Rh(CO)(H)(C$_7$H$_7$) absorbing at 2042 cm^{-1} also has biexponential kinetics, with a fast rise and a longer microsecond component that cannot be accurately determined from the data. The kinetics of the intermediate and final product is shown in Figure 5. These results indicate that bond activation in toluene and d_6-benzene occur by similar mechanisms.

The fact that the intermediates and product species in these arene C−H activation reactions have absorptions that are significantly shifted with respect to those of the intermediates η^2-Tp*Rh(CO)(solvents) and products η^3-Tp*Rh(CO)(H)(R) seen in the linear and cyclic hydrocarbon solvent data prompted us to measure the nanosecond spectra of the compound η^2-Bp*Rh(CO)$_2$ in d_6-benzene, as shown in Figure 6. These experiments were conducted as the photogenerated η^2-Bp*Rh(CO)(d_6-benzene) species provides a model for the dechelated intermediate η^2-Tp*Rh(CO)(d_6-benzene) which has been proposed to be responsible for the 2006 cm^{-1} absorption observed in the C−H activation studies. The results indicate that η^2-Bp*Rh(CO)(d_6-benzene) absorbs at 1993 cm^{-1}, similar to what has been observed in the linear and cyclic hydrocarbon data. These results call into question the nature of the intermediate state in these aryl C−H activation studies.

3. CpRh(CO)$_2$ in Linear Hydrocarbons. Shown in Figure 7 are the time-resolved difference IR spectra of CpRh(CO)$_2$ in *n*-pentane and *n*-hexane following UV excitation. At early times, the ultrafast spectra in *n*-pentane show the fast formation of

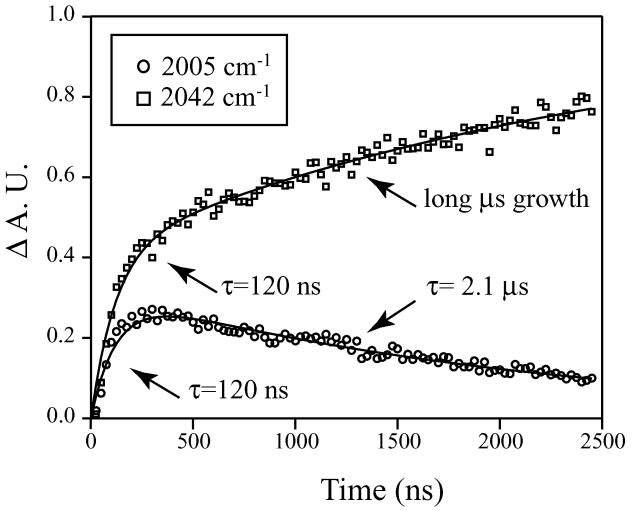

Figure 5. Ultrafast kinetics of the intermediate η^2-Tp*Rh(CO)(solvent) (circles) and product η^3-Tp*Rh(CO)(H)(R) (squares) in toluene. The time constants for the exponential fits (solid lines) are shown in the graph. (A. U. = arbitrary units.)

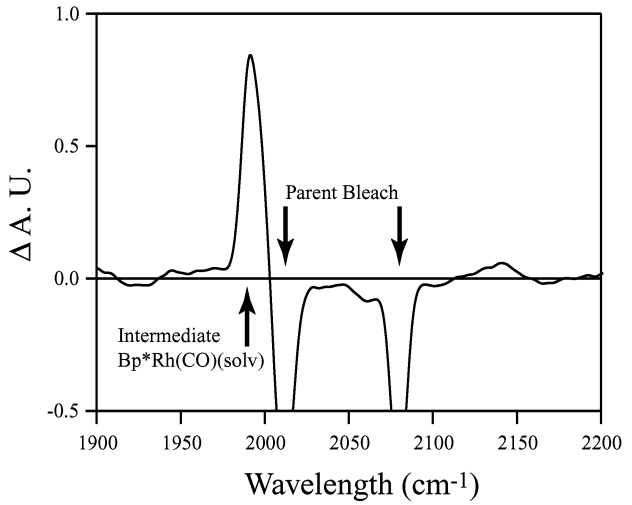

Figure 6. Transient difference spectrum in the CO stretching region for η^2-Bp*Rh$(CO)_2$ in neat d_6-benzene after UV photolysis. (A. U. = arbitrary units.)

the monocarbonyl alkyl solvate at 1963 cm^{-1} as well as two well-resolved hot bands of the parent CpRh$(CO)_2$ compound at 2020 and 2034 cm^{-1}, consistent with an earlier report.[51] These hot bands completely decay within 200 ps. At later times, the spectra indicate the formation of a new product absorbing at 2019 cm^{-1} with a corresponding decay of alkyl solvate. The species absorbing at 2019 cm^{-1} is assigned as the product CpRh(CO)(H)(C_5H_{11}), as its spectral position corresponds to that of the bond-activated product seen at 2016 cm^{-1} in the 50 ns spectrum in *n*-hexane. On the basis of the slight decay of the alkyl-solvated species, the rate of C−H activation of CpRh(CO)(*n*-pentane) is estimated to be 4.0×10^8 s^{-1} corresponding to a free energy barrier of 5.6 kcal/mol.

4. DFT Results. Theoretical chemical models have been shown to provide a wealth of information about C−H activation by transient metal complexes.[52−54] For this reason, these methods have been used to gain insight into the present study

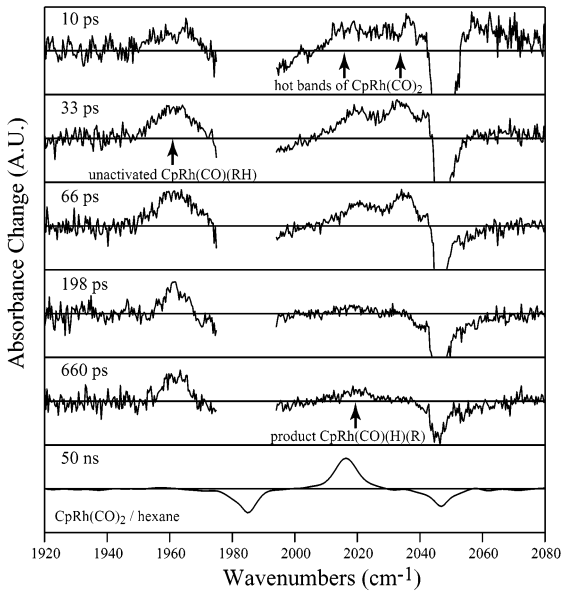

Figure 7. Transient difference spectra in the CO stretching region for CpRh$(CO)_2$ in neat *n*-pentane and *n*-hexane (50 ns spectrum) after UV photolysis. (A. U. = arbitrary units.)

of alkane and arene C−H activation. Shown in Figure 8 are the DFT-optimized structures of the proposed intermediate species η^2-Tp*Rh(CO)(benzene) and η^2-Tp*Rh(CO)(CH_4). The metal atom adopts a local square planar configuration when the Tp* ligand is coordinated in a bidentate fashion for both of the structures. The benzene substrate is bound to the metal via the C═C bond. The binding energies of the metal intermediate and the substrate have been found to be −15.3 kcal/mol for the benzene π-complex and −7.4 kcal/mol for the σ-complexed CH_4. A stable structure for the benzene C−H−Rh σ-type coordination could not be found when the Tp* ligand is partially dechelated, as our attempts to locate such a minimum resulted in the geometry converging to an η^3-Tp*Rh(CO)(σ-benzene) configuration. The optimized coordinates for these structures are provided in the Supporting Information.

Discussion

The results reported in this paper are consistent with those of earlier studies; the rate of C−H activation decreases from primary to secondary C−H bonds. Similar kinetic preferences have been observed in both CpRh$(CO)_2$ and η^3-Tp*Rh$(CO)_2$ in the present work. The results of the CpRh$(CO)_2$ data also clarify the role of ligand dynamics of the metal species in the bond activation reaction. The spectral data for all parent, product, and intermediate species are summarized in Table 1.

1. Linear versus Cyclic Hydrocarbon C−H Activation. The results of the *n*-pentane/cyclopentane and the *n*-hexane/cyclohexane studies with η^3-Tp*Rh$(CO)_2$ indicate that the activation process is faster with linear hydrocarbons, which have primary sites at the end of the alkane chain, than with ring hydrocarbons which have only secondary carbons. The CpRh$(CO)_2$ data also support this conclusion. One explanation for these results is that there may exist electronic structural differences between linear and cyclic hydrocarbons that account for the faster activation time scale in the former, regardless of

(51) Asbury, J. B.; Ghosh, H. N.; Yeston, J. S.; Bergman, R. G.; Lian, T. *Organometallics* **1998**, *17*, 3417.
(52) Musaev, D. G.; Morokuma, K. *J. Am. Chem. Soc.* **1995**, *117*, 799.
(53) Siegbahn, P. E. M. *J. Am. Chem. Soc.* **1996**, *118*, 1487.
(54) Niu, S.; Hall, M. B. *Chem. Rev.* **2000**, *100*, 353.

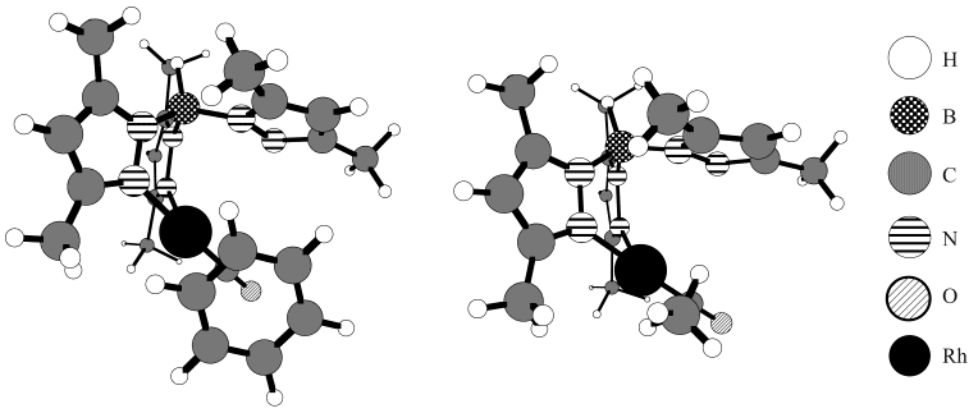

Figure 8. Geometries of the intermediate species η^2-Tp*Rh(CO)(CH_4) and η^2-Tp*Rh(CO)(C_6H_6) optimized at the DFT/B3LYP level of theory.

Table 1. Absorption Spectra of the Parents, Intermediates, and Product Species Observed in the Present Study

compound	frequency (cm^{-1})/solvent
η^3-Tp*Rh$(CO)_2$	1981, 2054/all hydrocarbons[b]
η^3-Tp*Rh(CO)(solvent)	1972/alkanes,[c] 1965/d_6-benzene
η^2-Tp*Rh(CO)(solvent)	1994/alkanes,[c] 2006/aromatic[d]
η^3-Tp*Rh(CO)(H)(R)	2028/alkanes,[c] 2042/aromatic[d]
η^2-Bp*Rh$(CO)_2$	2012, 2080/d_6-benzene
η^2-Bp*Rh(CO)(solvent)	1993/d_6-benzene
Cp*Rh$(CO)_2$	1985, 2048/*n*-pentane
Cp*Rh$(CO)_2$*[a]	2020, 2034/*n*-pentane
Cp*Rh(CO)(pentane)	1963/*n*-pentane
Cp*Rh(CO)(H)(R)	2019/*n*-pentane, 2016/*n*-hexane

[a] The data are for hot bands of the high-frequency CO absorption of the parent complex. [b] The parent absorptions are similar for linear, cyclic, and aromatic hydrocarbons. [c] The data for linear and cyclic hydrocarbons are generally similar. [d] The data presented are similar for d_6-benzene and toluene.

whether a primary or secondary site of the substrate is activated. A more likely reason is that C−H activation of linear hydrocarbons is occurring preferentially at the primary sites, reacting at a faster rate than C−H activation at secondary sites. Similar observations have been made in the reductive elimination studies of Northcutt et al., concluding that activation of primary C−H bonds is both kinetically and thermodynamically more favorable compared to secondary C−H activation of the same substrate.[13] Likewise, the rates of photochemical C−H activation by Cp*Rh$(CO)_2$ in linear and cyclic hydrocarbons measured by McNamara et al. are in agreement with the observation that C−H bond activation in a linear hydrocarbon occurs at a faster rate than that observed in the cyclic counterpart.[15] These observations may explain early synthetic results which found that activation in the final product occurs at the terminal primary C−H site of alkanes such as propane and hexane.[55,56] The data do not allow us, however, to determine whether C−H activation is occurring exclusively at primary C−H sites in linear hydrocarbons and some degree of secondary C−H activation likely occurs as well. The degree to which primary versus secondary C−H bonds are activated may be understood in context of the previous studies of Si−H activation in alkyl silanes, in which a dissociative intramolecular rearrangement mechanism was used to describe the formation of the Si−H activated product from less strongly bound alkyl solvates.[57,58] Consequently, a complex interplay of

Scheme 2. C−H Activation Mechanism of Cp*Rh$(CO)_2$ in Linear Hydrocarbons

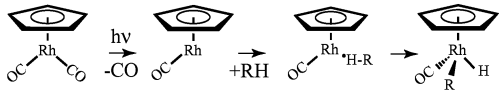

rearrangement, binding strength, and activation barrier is responsible for the observed kinetic traces.

The results of Tp*Rh$(CO)_2$ in methyl-cyclohexane show that product formation has similar kinetics as observed in linear alkanes, which is likely due to preferential activation of a primary methyl C−H bond despite the greater number of methylene secondary sites of the solvent. This result implies that the initially formed alkyl solvate can quickly rearrange to bind and activate the methyl group of the solvent. While we were not able to measure the isotope effect in aromatic solvents,[59] the activation of deuterated cyclohexane is slower by a moderate factor of 2.3 and is similar in magnitude to that observed in mechanistic studies using similar C−H-activating organometallic compounds.[60]

2. Ligand Dynamics of Cp*Rh$(CO)_2$ in C−H Activation. The role of ligand dynamics in the C−H activation reaction can be studied by comparing the reaction of Cp*Rh$(CO)_2$ to η^3-Tp*Rh$(CO)_2$ in alkanes. The ultrafast dynamics of Cp*Rh$(CO)_2$ in cyclohexane were previously studied by Asbury et al.[51] The results of these studies showed the exclusive formation of the alkyl solvate Cp*Rh(CO)(cyclohexane) with no evidence for the formation of the bond-activated product or a ring slipped intermediate within 500 ps. As the η^3-Tp*Rh$(CO)_2$ results above have shown that linear alkanes undergo bond activation at faster rates than their cyclic counterparts, we have investigated whether the reaction of Cp*Rh$(CO)_2$ in linear alkanes proceeds faster than in cyclohexane. The results are shown in Figure 7 and are summarized in Scheme 2. The spectral data of Cp*Rh$(CO)_2$ in *n*-pentane show the fast formation of the alkyl-solvated intermediate Cp*Rh(CO)(alkane) absorbing at 1963 cm^{-1} and two well-resolved vibrational hot bands of the parent which cool

(55) Jones, W. D.; Feher, F. J. *Organometallics* **1983**, *2*, 562.
(56) Wenzel, T. T.; Bergman, R. G. *J. Am. Chem. Soc.* **1986**, *108*, 4856.
(57) Yang, H.; Asplund, M. C.; Kotz, K. T.; Wilkens, M. J.; Frei, H.; Harris, C. B. *J. Am. Chem. Soc.* **1998**, *120*, 10154.
(58) Kotz, K. T.; Yang, H.; Snee, P. T.; Payne, C. K.; Harris, C. B. *J. Organomet. Chem.* **2000**, *596*, 183.
(59) The h_6-benzene and d_6-benzene results cannot be compared as the h_6-benzene solvent has absorptions that do not allow for the observation of the η^2-Tp*Rh(CO)(benzene) intermediate.
(60) Waltz, K. M.; Muhoro, C. N.; Hartwig, J. F. *Organometallics* **1999**, *18*, 3383.

Scheme 3. Si−H Bond Activation Mechanism of η^5-CpRh(CO)$_2$ in Triethylsilane[a]

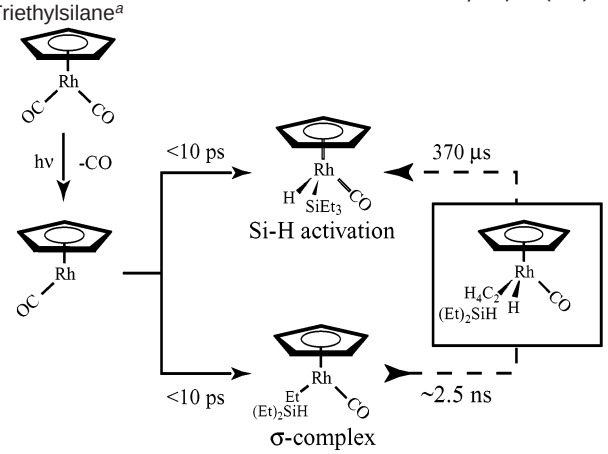

[a] The coordinatively unsaturated metal has been shown to activate the C−H bond of the alkyl-solvated intermediate. The time scale for formation of the product has been taken from ref 56.

within 200 ps. There is a 2.5 ns time scale decrease in the absorption of the alkyl-solvated intermediate with the concomitant formation of the bond-activated product seen at 2019 cm^{-1}. Consequently, there is no evidence for additional ligand dynamics in the C−H activation reaction such as the formation of ring slipped intermediates.[61] The observation of a bond-activated product in a linear hydrocarbon solvent on the ultrafast time scale shows that there is an increased barrier toward secondary versus primary photochemical C−H activation for CpRh(CO)$_2$.

A slight nanosecond time scale decay of the alkyl-solvated intermediate species was observed in our earlier study of Si−H activation of CpRh(CO)$_2$ in triethylsilane.[36] In light of our recent observation of C−H activation by CpRh(CO) in linear hydrocarbons, the previous result may now be attributed to C−H activation of the ethyl moiety of triethylsilane. The reaction mechanism of photochemical Si−H activation may be reformulated as shown in Scheme 3. Initially, the coordinatively unsaturated CpRh(CO) is solvated either by the Si−H bond to form the product or by the ethyl group to form the CpRh(CO)(Et)(SiHEt$_2$) intermediate. The C−H bond of the alkyl-solvated species is then activated to form a long-lived CpRh(CO)(H)(C$_2$H$_4$SiEt$_2$) intermediate, which eventually rearranges to form the final Si−H bond activated product along a 370 μs time scale.[62]

3. Arene C−H Activation. At early times, the activation of d_6-benzene by η^3-Tp*Rh(CO)$_2$ appears qualitatively similar to the results in linear and cyclic hydrocarbon solutions. Upon UV photolysis of η^3-Tp*Rh(CO)$_2$ in d_6-benzene, the picosecond spectra show the formation of a transient species absorbing at 1965 cm^{-1}, which decays within ~200 ps to form an intermediate absorbing at 2006 cm^{-1}. On the basis of the previous work, the first intermediate absorbing at 1965 cm^{-1} is proposed to be solvated η^3-Tp*Rh(CO)(benzene), which rearranges to form a dechelated η^2-Tp*Rh(CO)(benzene) intermediate. The 2.4 μs decay of η^2-Tp*Rh(CO)(benzene) is kinetically coupled to the long time scale growth component of the final η^3-Tp*Rh(CO)(D)(C$_6$D$_5$) product, which correlates to a free energy barrier of 9.6 kcal/mol.

While these assignments and general observations are in agreement with the mechanism seen in linear and cyclic alkanes, there are several important differences to note. First, the precursor complex has an increased lifetime in d_6-benzene compared to the η^2-Tp*Rh(CO)(solvent) intermediate seen in linear and cyclic hydrocarbon solutions. Also, the η^2-Tp*Rh(CO)(benzene) species absorption spectrum in d_6-benzene is ~15 cm^{-1} blue shifted with respect to the spectrum of the η^2 intermediate observed in linear and cyclic alkanes. The slower time scale for C−H activation in benzene might be due to rearrangement from a π-complex to a σ-solvated species before the reaction occurs. However, given the change in the spectrum of the intermediate and previous mechanistic studies which found evidence for the formation of C=C π-bound complexes as precursors to C−H activation,[20−25,28−30] the species absorbing at 2006 cm^{-1} is proposed to be a strongly bound η^2-Tp*Rh(CO)(π-benzene) which is solvated via the C=C double bond of d_6-benzene. These results are supported by our ab initio calculations, in which it was found that the binding strength of the η^2-Tp*Rh(CO)(π-benzene) complex is twice that of the methane substrate in the η^2-Tp*Rh(CO)(CH$_4$) intermediate. This proposal, however, is at odds with the photochemical experiments with the model precursor η^2-Bp*Rh(CO)$_2$ in d_6-benzene. The spectral data show a single absorption at 1993 cm^{-1} for η^2-Bp*Rh(CO)(benzene), the same as observed in linear and cyclic alkanes. These observations may be indicative of a greater degree of back-donation of the metal electron density to the aromatic substrate in the case of η^2-Tp*Rh(CO)(benzene) versus η^2-Bp*Rh(CO)(benzene).[63] At this stage, the discrepancy in the η^2-Bp*Rh(CO)$_2$ results cannot be rigorously accounted for, nor can the significant spectroscopic blue shifts in the intermediate and product η^3-Tp*Rh(CO)(D)(C$_6$D$_5$) absorptions relative to the counterparts in saturated hydrocarbon solvents. While we propose that the intermediate absorbing at 2006 cm^{-1} is the dechelated benzene π-complex, there appear to be more complex solute/solvent interactions in aromatic solvents than we are presently aware of.

The fact that the bond-activated product has biexponential kinetics indicates that there exist two possible routes to the formation of the bond-activated product. The fast component may be attributed to product formation of a Rh−D−C σ-bound species.[64] A similar observation has been made in the bond activation reaction of ethylene at the Cp*Ir[P(Me$_3$)] center [Cp* = C$_5$(CH$_3$)$_5$], in which the activation of the vinyl C−H bond proceeds not through a π-complex precursor but through a σ-complex.[23] The longer ~2 μs time scale component can be attributed to the decay of the π-complex to form the product as the two are kinetically coupled. Unfortunately, as a σ-complexed intermediate is not directly observed, it is impossible to tell if the Tp* ligand is dechelated into a bidentate form. Consequently, it is difficult to determine the total reaction mechanism of a σ-complex, as summarized in Scheme 4.

Results in toluene are similar to the d_6-benzene data. The intermediate and product peak positions are the same as in benzene, and the product growth occurs on a similar microsecond time scale. This is especially interesting as the cyclohexane and methyl-cyclohexane data indicate that the activation of the primary carbon is favored. Perhaps the formation of the

(61) Drolet, D. P.; Lees, A. J. *J. Am. Chem. Soc.* **1992**, *114*, 4186.
(62) Belt, S. T.; Grevels, F.-W.; Klotzbucher, W. E.; McCamley, A.; Perutz, R. N. *J. Am. Chem. Soc.* **1989**, *111*, 8373.
(63) Meiere, S. H.; Harman, W. D. *Organometallics* **2001**, *20*, 3876.
(64) This species does not appear to have been observed, and as such we are not certain whether the Tp* ligand is bound in an η^2 or in an η^3 fashion.

Scheme 4. C−H Bond Activation Mechanism of η^3-Tp*Rh(CO)$_2$ in Aryl Solvents[a]

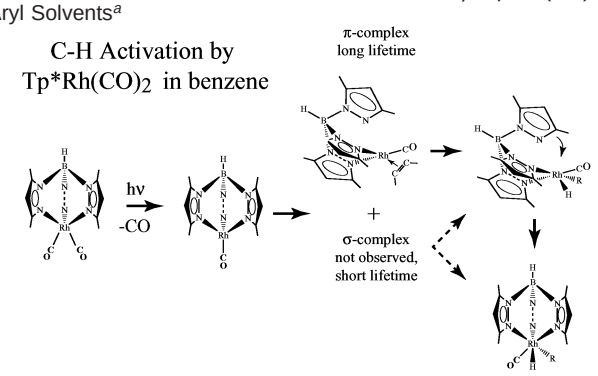

[a] It cannot be determined if the σ-complex exists as a dechelated intermediate, see text.

π-complex directs the reaction toward preferential activation at aromatic sites, as has been observed in previous activation studies using analogous compounds.[65] Consequently, while the unsaturated metal is able to bind and eventually activate the primary C−H bonds of the methyl-cyclohexane substrate, the strength of the bound π-complex precursor in toluene impedes such a rearrangement from occurring. The mechanism for aromatic C−H activation by η^3-Tp*Rh(CO)$_2$ is summarized in Scheme 4.

Conclusion

We have shown through direct observation that η^3-Tp*Rh(CO)$_2$ photochemically activates the C−H bonds of linear hydrocarbons at a faster rate than that seen for the substrates' cyclic counterparts. Experiments in methyl-cyclohexane solution suggest that this preference results in activation of the C−H bonds of the primary carbon despite the greater number of secondary sites of the solvent. The CpRh(CO)$_2$ studies also suggest that the same trend exists regardless of the local environment at the metal center. Further, the CpRh(CO)$_2$ data reveal that additional ligand dynamics do not appear to play a direct role in the photochemical activation process as has been established for η^3-Tp*Rh(CO)$_2$. The results of C−H activation studies in deuterated solvents by η^3-Tp*Rh(CO)$_2$ show a normal kinetic isotope effect of ~2.3 in the last step of the activation reaction.

In the case of photochemical activation in arene solvents, the formation of a strongly bound π-complex results in an increased time scale for C−H activation. In contrast to the methyl-cyclohexane data, the formation of a π-complex results in preferential activation of an aryl C−H bond in toluene. In both d_6-benzene and toluene, the kinetics of the bond-activated product is biexponential, which indicates that two routes exist to forming the final product. The fast component may be due to the reactivity of an unobserved σ-complexed intermediate which reacts at a rate similar to what has been observed in linear alkanes. The slow time scale product formation may be correlated with the decay of the η^2-Tp*Rh(CO)(π-benzene) intermediate.

Acknowledgment. C.B.H. thanks the National Science Foundation for funding. C.B.H, R.G.B., and H.F. are also supported by the Director, Office of Science, Office of Basic Energy Science, Chemical Sciences Division, under U.S. Department of Energy Contract DE-AC03-76SF00098.

Supporting Information Available: The optimized DFT structures of η^2-Tp*Rh(CO)(benzene) and η^2-Tp*Rh(CO)(CH$_4$) and the ultrafast UV pump/IR probe spectra of η^3-Tp*Rh(CO)$_2$ in d_6-benzene (PDF). This material is available free of charge via the Internet at http://pubs.acs.org.

JA020418S

(65) Bell, T. W.; Haddleton, D. M.; McCamley, A.; Partridge, M. G.; Perutz, R. N.; Willner, H. *J. Am. Chem. Soc.* **1990**, *112*, 9212.